PHOTONICS Research

Optical rogue wave in random fiber laser

JIANGMING XU,[1,3,†] JIAN WU,[1,†] JUN YE,[1] JIAXIN SONG,[1] BAICHENG YAO,[2] HANWEI ZHANG,[1] JINYONG LENG,[1] WEILI ZHANG,[2] PU ZHOU,[1,4] AND YUNJIANG RAO[2]

[1]College of Advanced Interdisciplinary Studies, National University of Defense Technology, Changsha 410073, China
[2]Fiber Optics Research Centre, Key Laboratory of Optical Fiber Sensing & Communications (Ministry of Education), University of Electronic Science & Technology of China, Chengdu 611731, China
[3]e-mail: jmxu1988@163.com
[4]e-mail: zhoupu203@163.com

Received 16 August 2019; revised 29 October 2019; accepted 29 October 2019; posted 1 November 2019 (Doc. ID 375481); published 6 December 2019

The famous demonstration of optical rogue waves (RWs), a powerful tool to reveal the fundamental physics in different laser scenarios, opened a flourishing time for temporal statistics. Random fiber laser (RFL) has likewise attracted wide attention due to its great potential in multidisciplinary demonstrations and promising applications. However, owing to the distinctive cavity-free structure, it is a scientific challenge to achieve temporal localized RWs in RFLs, whose feedback arises from multiple scattering in disordered medium. Here, we report the exploration of RW in the highly skewed, transient intensity of an incoherently pumped RFL for the first time, to our knowledge, and unfold the involved kinetics successfully. The corresponding frequency domain measurements demonstrate that the RW event arises from a crucial sustained stimulated Brillouin scattering process with intrinsic stochastic nature. This investigation highlights a novel path to fully understanding the complex physics, such as photon propagation and localization, in disordered media.

https://doi.org/10.1364/PRJ.8.000001

1. INTRODUCTION

The concept of random lasers employing multiple scattering of photons in an amplifying disordered material to achieve coherent light has attracted increasing attention due to features such as cavity-free structural simplicity and promising applications in imaging, medical diagnostics, and other scientific or industrial fields [1–3]. However, because of the lack of sharp resonances, it also has presented many challenges to conventional laser theory, such as light localization phenomenon in disordered amplifying media [4–6]. Random fiber laser (RFL), whose operation is based on the extremely weak Rayleigh scattering (RS) provided there is random distributed feedback in a piece of passive fiber, can trap the random laser radiation in a one-dimensional waveguide structure with efficiency and performance comparable to conventional fiber lasers [7,8]. It also presents rich physical properties in the spectral, temporal, and spatial domains [9–11]. In particular, the intensity fluctuation statistics (e.g., Lévy flights in output spectra) and involved dynamics have been extensively investigated in RFL as an important gateway to understand the operational mechanism and define features of the light source [12–19].

In general, intensity statistical investigations of fiber sources have flourished since the famous demonstration of optical rogue waves (RWs) [20,21]. Although the statistical RW behavior with (temporally or spatially) highly skewed intensity distributions and rare and unexpected appearance has been known for a long time in various different physical contexts such as oceanographic, capillary, and plasma waves and Bose–Einstein condensates (see, e.g., Ref. [22], for extensive reviews of this field), the optical RW phenomenon was only first presented in 2007 by Solli *et al.*, when they investigated the heavy-tailed histograms of intensity fluctuations in supercontinuum generation [20]. In recent years, the formation mechanisms of optical RWs have been determined both experimentally and theoretically in fiber lasers with nonlinearly driven cavities [20,23], Raman fiber lasers [24], and fiber lasers via modulation of the pump [25] (see the comprehensive overviews on this issue [26,27]). In contrast, up until now, the optical RW behavior with temporally localized structures has not been presented in RFLs with no defined cavity (or with an open cavity), even if the stochastic pulse shape originating from stimulated Brillouin scattering (SBS) has been observed in RFLs [7,28,29]. Detailed in the former RFLs constructed by a piece of common passive fiber, the SBS factor and associated giant pulses can only exist near the lasing threshold and will be suppressed in the power scalability (typically, about 25% higher than the lasing threshold in Ref. [7]) by the potential intensity fluctuations of pump laser, as discussed in Refs. [28,30]; otherwise, a section of special ultra-high numerical aperture (UHNA) passive fiber with small core diameter (usually about

2–4 μm) and limited conversion efficiency (about 10%) and robustness is necessary for the SBS stimulation [29]. Furthermore, despite the fact that the extreme event has been distinguished in random lasers around the threshold [14,31], there is no evidence as to the generation of optical RW. Consequently, the generation and evolution of optical RW behavior in RFLs has until now been an open issue.

In this work, we exploit a cavity-free structured RFL utilizing a simple experimental setup along with a piece of standard telecom fiber span and an incoherent amplified spontaneous emission (ASE) source. Thanks to the unique temporal stability property of pumping ASE light, the SBS process can be stimulated and sustained from nearly the lasing threshold to even maximal pump power (about 2.5 times higher than the lasing threshold). Simultaneously, optical RW behavior in an RFL is clearly demonstrated for the first time, to our knowledge, to occur both near and high above the lasing threshold transition. The exploration of optical RW behavior reveals the complex interplay processes, such as SBS, stimulated Raman scattering (SRS), and RS, in a cavity-free structured, incoherently pumped RFL. Our investigations may pave a new way to understand the fundamental physics underlying lasing from multiple scattering in one-dimensional disordered amplifying media, using an incoherently pumped RFL as the experimental platform.

2. EXPERIMENTAL SETUP AND RESULTS

A. Experimental Setup and Operating Principle

The proposed principle of the incoherently pumped self-pulsed RFL operation is depicted in Fig. 1. In brief, the RFL is primarily composed of a piece of 3.05 km long passive fiber (G.652, 8.2 μm core diameter, and 0.14 numerical aperture), with a total transmission loss of about 3 dB for pump light that is fused with one wavelength division multiplexer (WDM) for 1070/1120 nm. The end facets of passive fiber and pigtailed fiber of WDM are cleaved with angles of 8° and reflectivities of about 10^{-6} level to suppress the Fresnel reflections and ensure that the feedback is only provided by the distributed Rayleigh scattering in the passive fiber. The pump light we employed is an incoherent ASE source centered at 1063 nm, with a full width at half maximum (FWHM) linewidth of about 16 nm and unique little temporal fluctuation feature (more details can be found in Ref. [32]). The pump wave is injected into the passive fiber through the 1070 nm port of the WDM with an insertion loss of about 0.4 dB. It is well known that incident photons propagating in the long passive fiber can be backscattered by the random refractive index, inhomogeneity-induced weak RS and amplified by the SRS in this cavity-free RFL. Simultaneously, the acoustic field generated as a result of electrostriction can induce moving and stochastic density grating, which is defined as an SBS process [33,34]. Then, frequency downshifted photons owing to the Doppler effect will be stimulated with temporal transient characteristics. Consequently, a self-pulsed random laser can be achieved with the participation of the SBS effect.

Figures 2(a) and 2(b) illustrate the evolutions of output power and spectrum with the boosting of pump level, which clearly demonstrate the threshold behavior. Below the random

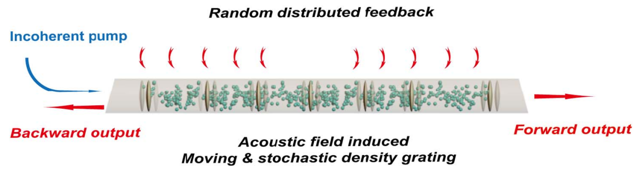

Fig. 1. Operating principle and output characteristics of the incoherently pumped random fiber laser (not to scale).

lasing threshold (about 6.11 W), most of the pump light is untransformed and transmitted to the forward direction, and the power of spontaneous Raman emission can be neglected, as plotted in Fig. 2(a). The spontaneous Raman emission spectrum is presented in Fig. 2(b), corresponding to an FWHM linewidth of about 12.54 nm. With the enhancing of pump power over threshold, random intense spikes localized around the Raman gain profile maxima (1120 nm) can be observed, which has a contrast of ∼30 dB against the spontaneous Raman emission pedestal. Simultaneously, due to the typical Schawlow–Townes spectral narrowing effect of random distributed feedback fiber lasers near the lasing threshold [9], the FWHM linewidth of the output spectrum dramatically decreases to an average value of 0.03 nm. Higher pumping results in the nonlinear increasing of output random laser power. With ultimate 21.29 W pump power employed (limited by the pump source), maximal output powers of 8.14 and 3.44 W can be obtained for the backward and forward first-order Stokes light, respectively. The backward first-order Stokes light power is significantly higher than that of forward output, which can be explained as follows. First, due to the higher pump power distribution near the backward output port, the Raman gain for the Stokes light is higher. Second, despite the fact that

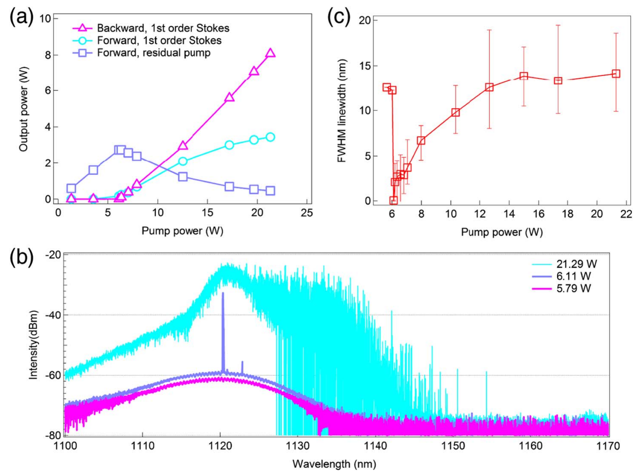

Fig. 2. Output characteristics of the incoherently pumped random fiber laser. (a) Output powers of first-order Stokes light and residual pump light as functions of pump power. (b) Typical spectra of the backward first-order Stokes light at different pump levels. The spectra are recorded with a resolution of 0.02 nm. (c) FWHM linewidth of backward spectral envelope as a function of injected pump power. The circles indicate the average FWHM linewidth of 20 measurements. The corresponding error bars mark the variation range of FWHM linewidth at fixed pump level.

Stokes light can be generated and amplified in both forward and backward directions, the forward Brillouin scattering in optical fiber is very weak, and hence the energy conversion from the pump light to the backscattered wave is more efficient [34]. As to the output spectrum, a broadband spectral envelope can be observed with mass characteristic spectral spikes even under the maximal operation power; the separations between spectral spikes are ∼0.06 nm, as expected for Stokes shifted SBS in 1 μm range [23]. Additionally, anti-Stokes components shorter than 1120 nm are also generated through the four-wave-mixing effect [35]. Furthermore, the spectral envelope varies from time to time with random spectral peaks and envelope linewidth, which can be attributed to the typical stochastic spectral behavior of the SBS effect [36], as the composed spectral peaks mainly originate from SBS scattering. To characterize the fluctuation of spectral envelope quantitatively, we depict the minimum, maximum, and mean values of 20 measurements in Fig. 2(c). Generally speaking, obvious spectral envelope broadening can be observed in the power-scaling process for nonlinear effects such as high-order SBS generation, self-phase modulation (SPM), and cross-phase modulation (XPM) [9]. Additionally, the statistical mean value of the FWHM linewidth evolves to a stable value of about 14 nm with the enhancement of pump power over 12.65 W.

B. Observation of Rogue Wave Behavior

As we know, pulsation operation can be obtained as the SBS factor can switch the Q value of RFL [29,37] and exist in the power boosting process. The evidence and evolution of the SBS effect will be given in the following with the aid of radiofrequency measurement at corresponding operation powers. To analyze the temporal characteristics of output pulsed random lasers, we employ a high-speed photodetector (45 GHz bandwidth) and a 16 GHz real-time oscilloscope with 100 MPts/channel capacity allowing us to record time series up to 32 ms with a 320 ps/point resolution. The typical temporal trace of the output random laser around threshold is recorded and plotted in Fig. 3(a), in which a large set of pulse clusters can be observed. The close-up view of the pulse bundle with the highest amplitude is plotted in Fig. 3(b). Induced by the intrinsic stochastic nature of the SBS effect, unstable pulsations are observed with random intervals, durations, and amplitudes. Furthermore, most of the pulses are so weak that they are nearly buried beneath the noise floor; however, the

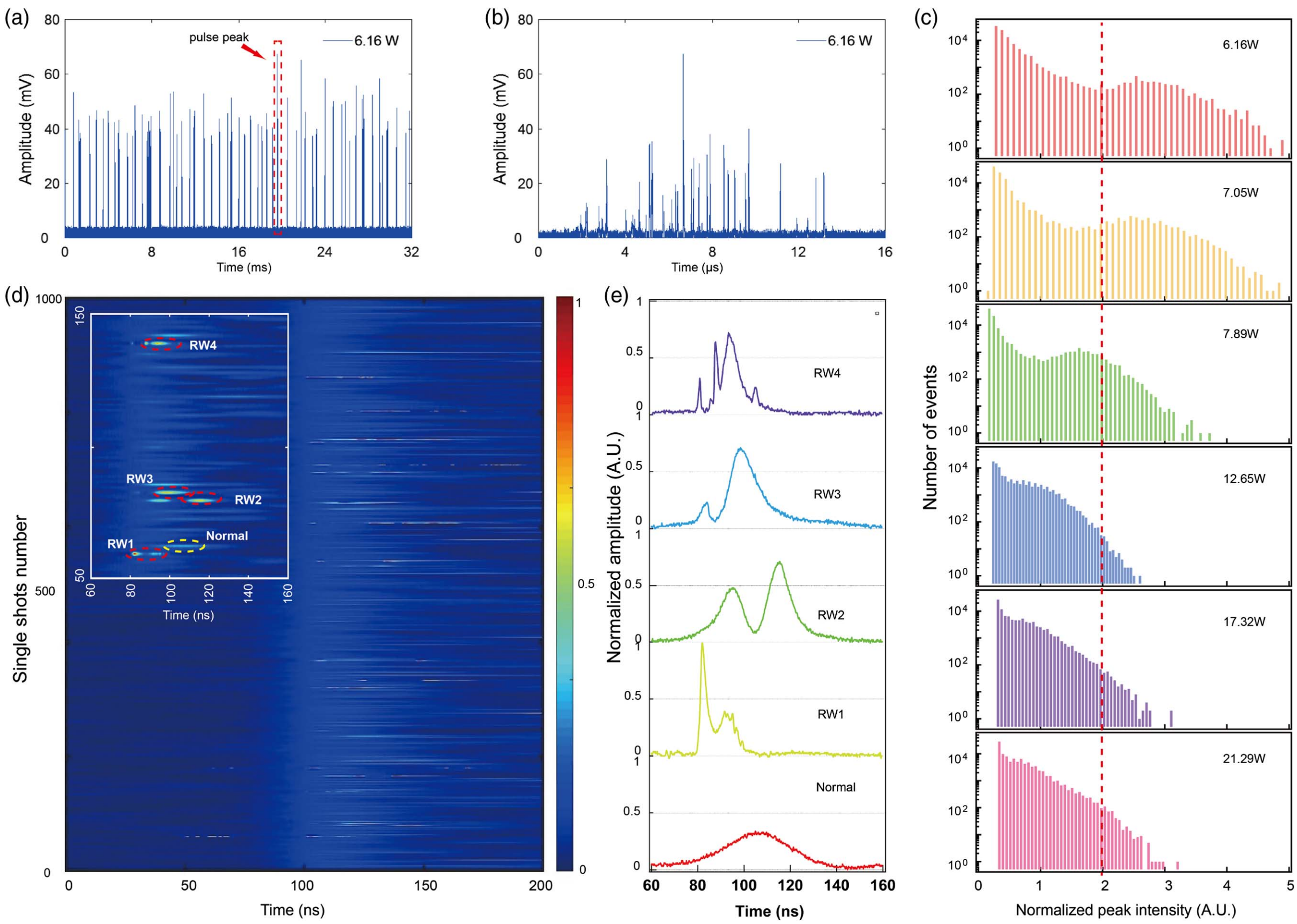

Fig. 3. Temporal characteristics and statistical features of output random laser. (a) and (b) Typical temporal trace of the output random laser around threshold. (c) Histograms (log scale) showing the distribution of optical intensity maxima for 10^5 trace events. The peak intensities are normalized by the corresponding SWH values. The vertical dashed lines indicate 2 × SWH and thus mark the limit for a pulse to be considered as an optical RW. (d) Evolution of consecutive traces around optical RW events at threshold. (e) Pulse shapes of typical normal and optical RW events.

largest pulses can reach intensities about 20 times that of the lowest ones.

To check whether the RWs are generated or not in this self-pulsed RFL, we measured and recorded the peak amplitude of the shot-to-shot nanosecond pulse and added it to a histogram. The measurement and recording are similar to those in Ref. [38] and were automatically repeated at a rate of about 2×10^5 trace samples per hour. Figure 3(c) presents the statistical distribution histograms recorded for the peak amplitudes of 10^5 consecutive traces corresponding to different pump levels. Additionally, the vertical dashed line indicates a peak amplitude twice the significant wave height (SWH, defined as the mean height of the highest third of events [39]) of each measurement, and denotes the calculated amplitude from which events are considered RWs. It should be noted that the peak amplitudes, shown as the horizontal axis of Fig. 3(c), are normalized by corresponding SWHs to investigate the proportion evolution of RW in the power boosting more conveniently. The heavy-tailed histograms display numerous events, with peak amplitudes more than twice the SWH, thus revealing the generation of RW behavior in this self-pulsed RFL.

Unlike the intensity fluctuations following a Gaussian probability distribution of a laser above threshold, the output random laser of this incoherently pumped RFL is featured with long-tailed distribution for the intrinsic stochastic nature of the SBS process, as it is well-known that a nonlinear transfer function (e.g., SBS process) can modify the probability distribution of an input light [39]. Furthermore, around the threshold, the highest recorded peak amplitudes can reach intensity about 5 times that of the corresponding SWH, and the emergence proportion of RW events is about 4.1%. As the pump power increases, the RW events can always be observed, even at maximal power level. However, the peak amplitude and generation probability decrease to stable values of ~3 times that of SWH and 0.35%, respectively. These decrements may be induced by the denser nanosecond pulses and associated higher SWH value. To show the trend of RW event generation in this self-pulsed RFL at 6.16 W pump level, the shot pulse evolution over 1000 consecutive traces and typical enlarged view around RW events are depicted in Fig. 3(d). First, due to the stochastic nature of SBS, the recorded traces suffer from shot-to-shot perturbations. Thus, there are rare high-amplitude traces with peak intensities higher than twice the SWH, which are also generated unpredictably and disappear with a transient state. Indeed, these agree well with the criteria of RW behavior [38,40]. The typical pulse shapes of normal and RW events, illustrated by Fig. 3(e), also indicate the high fluctuation and multiplicity of pulse duration and amplitude of RW events. Furthermore, the pulse width of the observed RW event (several nanoseconds to tens of nanoseconds) is much shorter than the transmitted time (μs range) in the passive fiber. Hence, we can infer that the observed RW events are fast RW [17,18].

The long-term power stabilities of output lasers and injected pump light, as depicted in Fig. 4, are measured by power meters with 1 s/point resolution and half-hour recorded length. First, contrasted with the unstable nanosecond pulsations with RW characteristics induced by the intrinsic stochastic nature of the SBS effect, the average powers of output lasers indicate

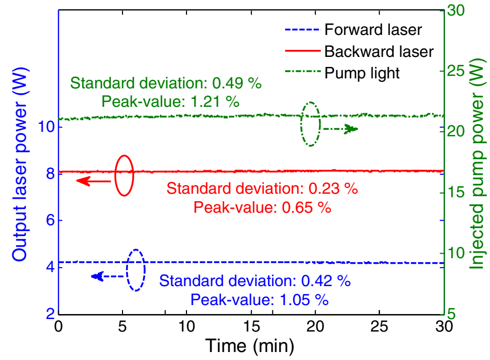

Fig. 4. Long-term average power stabilities of output lasers and injected pump. The average powers are measured by power meters with 1 s/point resolution and half-hour recorded length.

good long-term power stabilities, which may benefit from the employment of an ultra-stable ASE source as the pump light [32]. This situation is somewhat similar to the classical physical problem in which long-term average properties of the system are determined by the random behavior of a huge number of waves [41]. Furthermore, the measurements indicate that the intensity fluctuations of the output random laser are not correlated with fluctuation of the pump light in the long-term range. In a way, the power stability of the generated random laser is superior to that of the employed pump light. Generally speaking, this incoherently pumped self-pulsed RFL exhibits good long-term average power stabilities at quasi-hour scale and giant pulse behaviors, with RW characteristics at nanosecond scale simultaneously.

C. Radio Frequency Evolution of Self-Pulsed RFL

To investigate the self-pulsed operation dynamics and confirm the generation of the SBS effect, we measure the radio frequency (RF) evolution of the output random laser, as depicted in Fig. 5. From the lasing threshold to the maximal pump level, a well-pronounced beating peak near 15 GHz, which coincides with the Brillouin frequency shift ($\Delta\nu_B = 2n\nu_a/\lambda$, where n, ν_a, and λ are respectively the refractive index, velocity of acoustic wave, and pump wavelength of the SBS process) of the laser around 1120 nm in the passive fiber [23,34] can always be measured clearly, indicating the presence of SBS effect in the power boosting process. Additionally, Fig. 5(b) shows enlarged views around the 15 GHz characteristic peak. The mutation in the noise floor trace is induced by the electrical signal amplifier of the RF analyzer. At the lasing threshold, independent peaks can be observed with >30 dB signal-to-noise ratio (SNR) for the highest signal. However, with the scaling of pump power to 7.05 W, the RF spectroscopy develops more components at new frequencies, which is similar to that in Ref. [42], and evolves to a quasi-cw shape with little fluctuations. In the boosting of pump power from 7.05 W to the maximal 21.29 W, the gain magnification of the low-frequency section (lower than ~15 GHz) in the RF spectrum is superior to that of the high-frequency section with respect to the cascaded SBS-generated long-wavelength components and corresponding lower RF frequency (as indicated by the formula before). At the maximum pump level, the 10 dB width of the

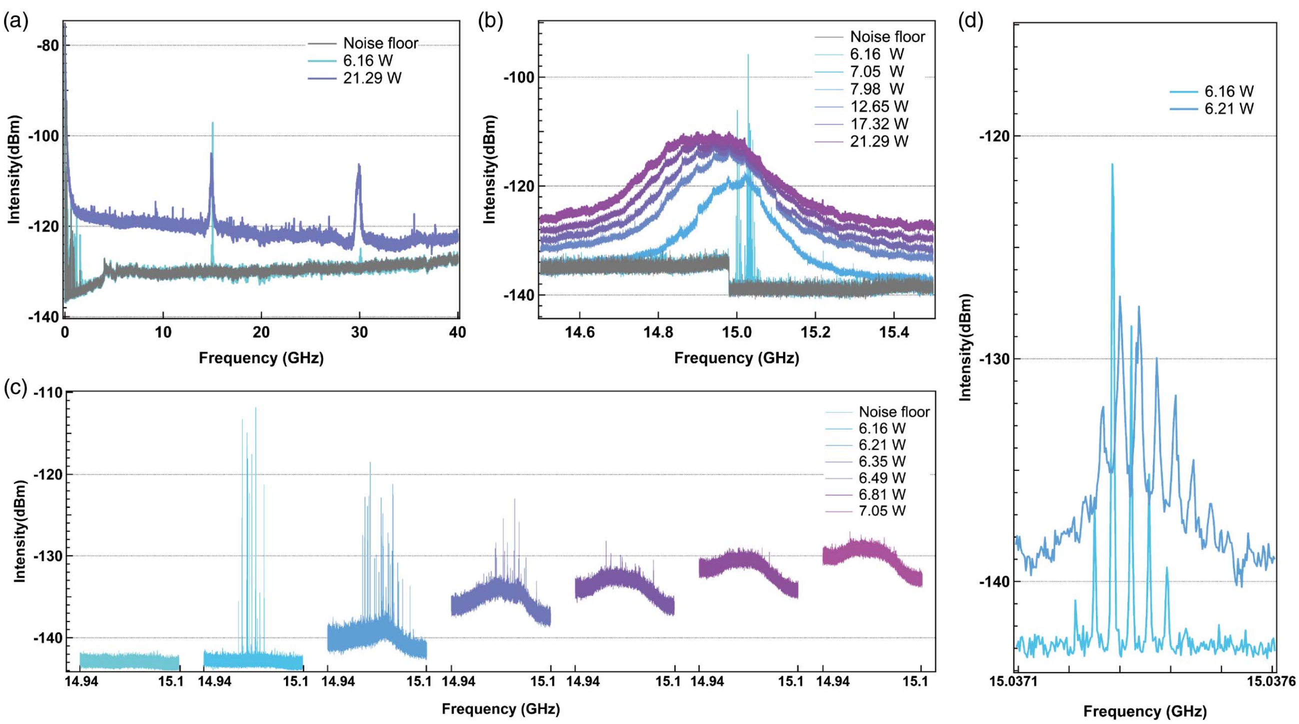

Fig. 5. RF spectra of output random laser. (a) Long-span RF spectra (measured with a resolution of 1 kHz). (b) RF spectral envelopes corresponding to SBS effect (recorded with a resolution of 10 Hz). (c) Evolution of spectra from mass independent peaks to quasi-cw envelopes (measured with a resolution of 1 Hz). (d) Enlarged view of selected RF peaks around the lasing threshold.

broadband RF spectral envelope is about 285 MHz (14.725 to 15.110 GHz), corresponding to the wavelength from 1142.91 to 1113.79 nm. This RF spectroscopy measurement coincides well with the former optical spectrum test plotted in Fig. 2(b).

Additionally, we investigate the RF spectrum evolution around the characteristic frequency corresponding to the SBS effect from mass independent peaks to quasi-cw spectral envelope, as charted in Figs. 5(c) and 5(d), and find the coexistence states of these two typical RF spectra. The amplitudes of the quasi-cw spectral pedestal and signal peak increase and decrease gradually and inversely with the enhancing of pump power from threshold to 7.05 W. Additionally and surprisingly, specific fine structures with frequency interval of about 36 kHz can be found around the lasing threshold, as displayed in Fig. 5(d). As the previous investigations had indicated that the RFL can present rich kinetics around the lasing threshold [7,43], and the localization mechanism can induce a localized ordered operation state in disordered medium [44–47], this fine structure may be another localization-dynamic-induced threshold behavior in RFL. The conversion of RF spectrum to quasi-cw spectral envelope may be explained as follows. Despite the fact that only independent peaks are generated at the lasing threshold, with the pump power scaling, multiple nonlinear [28] interactions (such as four-wave-mixing and self-phase and cross-phase modulations) and associated spectral broadening can generate new wavelength components as the pump light of SBS processes and bridges the gaps between the independent peaks. As the characteristic RF peaks near 15 GHz are relevant to the pump wavelength of the SBS process in the passive fiber, indicated by the former Brillouin frequency shift formula, the gap bridging of the pump spectrum can also smooth the RF spectrum and induce the envelope. In hence, with the aid of cascaded SBS process and multiple nonlinear effects, the mass independent peaks at the lasing threshold can evolve to the quasi-cw spectral envelope gradually with the power scalability.

3. DISCUSSION

Note that the SBS effect had been observed in many RFLs constructed by common passive fiber in past years [7,37]. Furthermore, the previous literature had indicated that with SBS effect and the associated irregular giant pulses, spiky optical spectrum could be suppressed with the scalability of pump power overcoming the lasing threshold [7,28,30] (e.g., about 25% higher than lasing threshold in Ref. [7]). This was attributed to the pump laser intensity fluctuation-induced phase fluctuations and corresponding optical spectral broadening via the cross-phase modulation process [7,28,30]. Nevertheless, in this RFL pumped by an incoherent ASE source with an FWHM linewidth as broad as about 16 nm, the SBS factor was sustained from the lasing threshold to even the maximal pump level (21.29 W), which is about 2.5 times higher than the threshold. The most probable reason for this is the use of ASE source with high temporal stability [32] as a pump source. This compact high-power RFL with RW characteristics can provide a pulsed light source for many applications, such as supercontinuum generation. Furthermore, apart from the identification of stochastic pulses with large pulse-to-pulse intensity fluctuations and associated spiky spectrum, the previous investigations did not reveal any RW behavior in such SBS-assisted self-Q-switched RFL platforms [7,29,37]. Here, the temporal statistics measurement shows the RW characteristics of this self-pulsed RFL for the first time to our knowledge. The RW events can also be observed even at maximal pump power, with peak amplitudes of about 3 times the corresponding SWH value. However, we cannot simulate the self-pulsing operation regime involving cooperative RS–SRS–SBS processes in this RFL presently, due to the enormous computation induced by the complex interactions between different components, relatively long (kilometer-level) passive fiber, and transient nanosecond-level pulse duration demanding precise time steps. This will be our next goal.

4. SUMMARY

In conclusion, we have shown an incoherently pumped RFL with optical RW behavior induced by the intrinsic stochastic nature of the SBS effect under even maximal pump power (about 2.5 times higher than the lasing threshold). This is the first presentation of optical RW characteristic in RFL, to the best of our knowledge, and our investigation could pave a new way to reveal the fundamental physical dynamics underlying the operation and performance of random lasers in disordered media. Further statistical and analytical studies are necessary to characterize the remarkably challenging complex phenomena in this RFL, involving cascaded nonlinear interactions such as RS–SRS–SBS cooperative processes.

Funding. National Natural Science Foundation of China (61322505, 61905284, 61635005); National Postdoctoral Program for Innovative Talents (BX20190063); 111 Project of China (B14039); Huo Ying Dong Education Foundation of China (151062); Natural Science Foundation of Hunan Province (2018JJ03588).

Acknowledgment. We are particularly grateful to Prof. Z. C. Luo and Dr. M. Liu from South China Normal University for their elicited and useful discussions.

[†]These authors contributed equally to this work.

REFERENCES

1. R. Ambartsumyan, N. Basov, P. Kryukov, and V. Letokhov, "A laser with a nonresonant feedback," IEEE J. Quantum Electron. **2**, 442–446 (1966).
2. N. M. Lawandy, R. M. Balachandran, A. S. L. Gomes, and E. Sauvain, "Laser action in strongly scattering media," Nature **368**, 436–438 (1994).
3. D. S. Wiersma, "The physics and applications of random lasers," Nat. Phys. **4**, 359–367 (2008).
4. V. Milner and A. Z. Genack, "Photon localization laser: low-threshold lasing in a random amplifying layered medium via wave localization," Phys. Rev. Lett. **94**, 073901 (2005).
5. H. E. Türeci, L. Ge, S. Rotter, and A. D. Stone, "Strong interactions in multimode random lasers," Science **320**, 643–646 (2008).
6. B. Abaie, E. Mobini, S. Karbasi, J. Ballato, and A. Mafi, "Random lasing in an Anderson localizing optical fiber," Light Sci. Appl. **6**, e17041 (2017).
7. S. K. Turitsyn, S. A. Babin, A. E. El-Taher, P. Harper, D. V. Churkin, S. I. Kablukov, J. D. Ania-Castañón, V. Karalekas, and E. V. Podivilov, "Random distributed feedback fibre laser," Nat. Photonics **4**, 231–235 (2010).
8. D. V. Churkin, S. Sugavanam, I. D. Vatik, Z. Wang, E. V. Podivilov, S. A. Babin, Y. Rao, and S. K. Turitsyn, "Recent advances in fundamentals and applications of random fiber lasers," Adv. Opt. Photon. **7**, 516–569 (2015).
9. D. V. Churkin, I. V. Kolokolov, E. V. Podivilov, I. D. Vatnik, M. A. Nikulin, S. S. Vergeles, I. S. Terekhov, V. V. Lebedev, G. Falkovich, S. A. Babin, and S. K. Turitsyn, "Wave kinetics of random fibre lasers," Nat. Commun. **6**, 6214 (2015).
10. I. R. R. González, B. C. Lima, P. I. R. Pincheira, A. A. Brum, A. M. S. Macêdo, G. L. Vasconcelos, L. de S. Menezes, E. P. Raposo, A. S. L. Gomes, and R. Kashyap, "Turbulence hierarchy in a random fibre laser," Nat. Commun. **8**, 15731 (2017).
11. W. Pan, L. Zhang, H. Jiang, X. Yang, S. Cui, and Y. Feng, "Ultrafast Raman fiber laser with random distributed feedback," Laser Photon. Rev. **12**, 1700326 (2018).
12. A. S. L. Gomes, E. P. Raposo, A. L. Moura, S. I. Fewo, P. I. R. Pincheira, V. Jerez, L. J. Q. Maia, and C. B. de Araújo, "Observation of Lévy distribution and replica symmetry breaking in random lasers from a single set of measurements," Sci. Rep. **6**, 27987 (2016).
13. B. C. Lima, A. S. L. Gomes, P. I. R. Pincheira, A. L. Moura, M. Gagné, E. P. Raposo, C. B. de Araújo, and R. Kashyap, "Observation of Lévy statistics in one-dimensional erbium-based random fiber laser," J. Opt. Soc. Am. B **34**, 293–299 (2017).
14. B. C. Lima, P. I. R. Pincheira, E. P. Raposo, L. d. S. Menezes, C. B. de Araújo, A. S. L. Gomes, and R. Kashyap, "Extreme-value statistics of intensities in a cw-pumped random fiber laser," Phys. Rev. A **96**, 013834 (2017).
15. L. L. Ogorodnikov and S. S. Vergeles, "Intensity statistics in a long random fiber Raman laser," Opt. Lett. **43**, 651–654 (2018).
16. J. Li, H. Wu, Z. Wang, S. Lin, C. Lu, E. P. Raposo, A. S. L. Gomes, and Y. Rao, "Lévy spectral intensity statistics in a Raman random fiber laser," Opt. Lett. **44**, 2799–2802 (2019).
17. S. A. Kolpakov, H. Kbashi, and S. V. Sergeyev, "Dynamics of vector rogue waves in a fiber laser with a ring cavity," Optica **3**, 870–875 (2016).
18. S. V. Sergeyev, S. A. Kolpakov, C. Mou, G. Jacobsen, S. Popov, and V. Kalashnikov, "Slow deterministic vector rogue waves," Proc. SPIE **9732**, 97320K (2016).
19. S. V. Sergeyev, H. Kbashi, N. Tarasov, Y. Loiko, and S. A. Kolpakov, "Vector-resonance-multimode instability," Phys. Rev. Lett. **118**, 033904 (2017).
20. D. R. Solli, C. Ropers, P. Koonath, and B. Jalali, "Optical rogue waves," Nature **450**, 1054–1057 (2007).
21. A. Klein, G. Masri, H. Duadi, K. Sulimany, O. Lib, H. Steinberg, S. A. Kolpakov, and M. Fridman, "Ultrafast rogue wave patterns in fiber lasers," Optica **5**, 774–778 (2018).
22. M. Onorato, S. Residori, U. Bortolozzo, A. Montina, and F. T. Arecchi, "Rogue waves and their generating mechanisms in different physical contexts," Phys. Rep. **528**, 47–89 (2013).
23. P. H. Hanzard, M. Talbi, D. Mallek, A. Kellou, H. Leblond, F. Sanchez, T. Godin, and A. Hideur, "Brillouin scattering-induced rogue waves in self-pulsing fiber lasers," Sci. Rep. **7**, 45868 (2017).
24. A. F. J. Runge, C. Aguergaray, N. G. R. Broderick, and M. Erkintalo, "Raman rogue waves in a partially mode-locked fiber laser," Opt. Lett. **39**, 319–322 (2014).
25. A. N. Pisarchik, R. Jaimes-Reátegui, R. Sevilla-Escoboza, G. Huerta-Cuellar, and M. Taki, "Rogue waves in a multistable system," Phys. Rev. Lett. **107**, 274101 (2011).
26. N. Akhmediev, J. M. Dudley, D. R. Solli, and S. K. Turitsyn, "Recent progress in investigating optical rogue waves," J. Opt. **15**, 060201 (2013).
27. N. Akhmediev, B. Kibler, F. Baronio, M. Belić, W.-P. Zhong, Y. Zhang, W. Chang, J. M. Soto-Crespo, P. Vouzas, P. Grelu, C. Lecaplain, K. Hammani, S. Rica, A. Picozzi, M. Tlidi, K. Panajotov, A. Mussot, A. Bendahmane, P. Szriftgiser, G. Genty, J. Dudley, A. Kudlinski, A. Demircan, U. Morgner, S. Amiraranashvili, C. Bree, G. Steinmeyer, C. Masoller, N. G. R. Broderick, A. F. J. Runge, M. Erkintalo, S. Residori, U. Bortolozzo, F. T. Arecchi, S. Wabnitz, C. G. Tiofack,

S. Coulibaly, and M. Taki, "Roadmap on optical rogue waves and extreme events," J. Opt. **18**, 063001 (2016).
28. D. V. Churkin, S. A. Babin, A. E. El-Taher, P. Harper, S. I. Kablukov, V. Karalekas, J. D. Ania-Castañón, E. V. Podivilov, and S. K. Turitsyn, "Raman fiber lasers with a random distributed feedback based on Rayleigh scattering," Phys. Rev. A **82**, 033828 (2010).
29. Y. Tang and J. Xu, "A random *Q*-switched fiber laser," Sci. Rep. **5**, 9338 (2015).
30. S. K. Turitsyn, S. A. Babin, D. V. Churkin, I. D. Vatnikc, M. Nikulinc, and E. V. Podivilov, "Random distributed feedback fibre lasers," Phys. Rep. **542**, 133–193 (2014).
31. R. Uppu and S. Mujumdar, "Physical manifestation of extreme events in random lasers," Opt. Lett. **40**, 5046–5049 (2015).
32. J. Xu, L. Huang, J. Leng, H. Xiao, S. Guo, P. Zhou, and J. Chen, "1.01 kW superfluorescent source in all-fiberized MOPA configuration," Opt. Express **23**, 5485–5490 (2015).
33. Z. Zhu, D. J. Gauthier, and R. W. Boyd, "Stored light in an optical fiber via stimulated Brillouin scattering," Science **318**, 1748–1750 (2007).
34. A. Kobyakov, M. Sauer, and D. Chowdhury, "Stimulated Brillouin scattering in optical fibers," Adv. Opt. Photon. **2**, 1–59 (2010).
35. J. W. Lou, F. K. Fatemi, and M. Currie, "Brillouin fibre laser enhanced by Raman amplification," Electron. Lett. **40**, 1044–1046 (2004).
36. M. Salhi, A. Hideur, T. Chartier, M. Brunel, G. Martel, C. Ozkul, and F. Sanchez, "Evidence of Brillouin scattering in an ytterbium-doped double-clad fiber laser," Opt. Lett. **27**, 1294–1296 (2002).
37. G. Ravet, A. A. Fotiadi, M. Blondel, and P. Mégret, "Passive *Q*-switching in all-fibre Raman laser with distributed Rayleigh feedback," Electron. Lett. **40**, 528–529 (2004).
38. C. Lecaplain, P. Grelu, J. M. Soto-Crespo, and N. Akhmediev, "Dissipative rogue waves generated by chaotic pulse bunching in a mode-locked laser," Phys. Rev. Lett. **108**, 233901 (2012).
39. J. M. Dudley, F. Dias, M. Erkintalo, and G. Genty, "Instabilities, breathers and rogue waves in optics," Nat. Photonics **8**, 755–764 (2014).
40. C. Bonatto, M. Feyereisen, S. Barland, M. Giudici, C. Masoller, J. Leite, and J. Tredicce, "Deterministic optical rogue waves," Phys. Rev. Lett. **107**, 053901 (2011).
41. S. K. Turitsyn, J. D. Ania-Castañón, S. A. Babin, V. Karalekas, P. Harper, D. Churkin, and V. K. Mezentsev, "270-km ultralong Raman fiber laser," Phys. Rev. Lett. **103**, 133901 (2009).
42. P. Dainese, P. S. J. Russell, N. Joly, J. C. Knight, G. S. Wiederhecker, H. L. Fragnito, V. Laude, and A. Khelif, "Stimulated Brillouin scattering from multi-GHz-guided acoustic phonons in nanostructured photonic crystal fibres," Nat. Phys. **2**, 388–392 (2006).
43. S. Sugavanam, M. Sorokina, and D. V. Churkin, "Spectral correlations in a random distributed feedback fibre laser," Nat. Commun. **8**, 15514 (2017).
44. V. M. Apalkov, M. E. Raikh, and B. Shapiro, "Random resonators and prelocalized modes in disordered dielectric films," Phys. Rev. Lett. **89**, 016802 (2002).
45. J. Andreasen, A. A. Asatryan, L. C. Botten, M. A. Byrne, H. Cao, L. Ge, L. Labonté, P. Sebbah, A. D. Stone, H. E. Türeci, and C. Vanneste, "Modes of random lasers," Adv. Opt. Photon. **3**, 88–127 (2011).
46. A. Mafi, "Transverse Anderson localization of light: a tutorial," Adv. Opt. Photon. **7**, 459–515 (2015).
47. G. Ruocco, B. Abaie, W. Schirmacher, A. Mafi, and M. Leonetti, "Disorder-induced single-mode transmission," Nat. Commun. **8**, 14571 (2017).